Corrosion Inhibition of Aluminum with a 3-(10-Sodium sulfonate decyloxy) Aniline Monomeric Surfactant and Its Analog Polymer in a 0.5*M* Hydrochloric Acid Solution

M. M. El-Deeb, S. M. Mohamed

Chemistry Department, Faculty of Science, Beni Suef University, Beni Suef 62514, Egypt

ABSTRACT: The inhibitory effect of a 3-(10-sodium sulfonate decyloxy) aniline monomeric surfactant and the analog polymeric surfactant poly[3-(decyloxy sulfonic acid) aniline] (PC_{10}) on the corrosion of aluminum in 0.5*M* hydrochloric acid was studied with weight loss and potentiodynamic polarization techniques. The results show that the inhibition occurred through the adsorption of inhibitor molecules on the metal surface. The inhibition efficiency was found to increase with increasing inhibitor concentration and decrease with increasing temperature. It was found that these inhibitors acted as mixed-type inhibitors with anodic predominance. The adsorption of these compounds on the metal surface obeyed the Langmuir and Frumkin adsorption isotherms. Thermodynamic functions for both the dissolution and adsorption processes were determined. The obtained results from the weight loss and potentiodynamic polarization techniques were in a good agreement. © 2011 Wiley Periodicals, Inc. J Appl Polym Sci 122: 3030–3037, 2011

Key words: activation energy; adsorption; conducting polymers; electrochemistry; surfactants

INTRODUCTION

Aluminum (Al) finds a wide spread spectrum of technological applications because of its particular properties, including its low density, good appearance, and corrosion resistance. For these reasons, the corrosion behavior of Al has attracted the attention of many investigators.[1–7] Hydrochloric acid solutions are used for pickling and chemical and electrochemical etching of Al and its alloys. It is very important to add a corrosion inhibitor to decrease the corrosion rate of Al in such solutions. Several authors[1–4] have studied the corrosion inhibition of Al and its alloys by organic inhibitors in acid solutions. Various aliphatic and aromatic amines and nitrogen heterocyclic compounds have been applied as corrosion inhibitors for Al in acid media.[5–9] Hydrazine compounds,[10–12] organic acids, and their salts,[13] dicyandiamide and some of its related compounds,[14] ethoxylated fatty acids,[15] and Schiff bases[16] have also been found to inhibit the corrosion of Al in a hydrochloric acid (HCl) solution.

The adsorption of a surfactant on a metal surface can markedly change the corrosion-resistance properties of the metal.[17,18] Therefore, the study of relation between the adsorption and corrosion inhibition is of great importance. Recently, many surfactants have been widely used as corrosion inhibitors for some metals and alloys in cleaning, pickling, and waterborne printing inks processes.[19–22]

Water-soluble polymeric compounds have attracted great interest as corrosion inhibitors for different metals in different media.[23–26] Polyvinylpyrrolidone has received particular attention and has been applied to the inhibition of Al in hydrochloric acid solution.[25]

In this work, the effect of a novel inhibitor, a 3-(10-sodium sulfonate decyloxy) aniline (MC_{10}) monomeric surfactant, and its analog polymer, a poly[3-(decyloxy sulfonic acid) aniline] (PC_{10}) polymeric surfactant, on the corrosion behavior of Al in an acid medium was investigated in different concentrations and temperatures with weight-loss, potentiodynamic polarization methods. Also, the thermodynamic functions for the dissolution and adsorption were investigated. Careful examination of the literature revealed that the studied polysurfactant had not yet been studied as a corrosion inhibitor.

EXPERIMENTAL

Materials

3-Aminophenol, potassium persulfate, and 1,10-dibromodecane were obtained from Aldrich Chemical Co. (England). Sodium sulfite, used in the

Correspondence to: M. M. El-Deeb (eldeebm@yahoo.com).

TABLE I
Elemental Analyses of MC_{10} and Its Analog PC_{10}

Surfactant	C (%)		H (%)		Cl (%)		S (%)		N (%)		Na (%)	
	Calcd	Found	Calcd	Found	Calcd	Found	Calcd	Found	Calcd	Found	Calcd	Found
MC_{10}	54.70	54.12	7.41	7.32	—	—	9.12	8.98	3.99	3.61	6.55	6.28
PC_{10}	53.74	52.96	4.90	4.74	8.97	8.73	8.96	8.75	3.96	3.72	—	—

synthetic process, was obtained from Merck Chemical, Ltd. (Darmstadt, Germany). Pure-grade HCl was provided by Prolabo Chemical Co. (England).

Weight-loss measurements

Al metal was provided by the Egyptian Aluminum Co. (Nag Hammady, Egypt) with dimensions of $2 \times 2 \times 0.1$ cm^3, with a chemical composition of 99.57 wt % Al, 0.31 wt % Fe, 0.07 wt % Si, 0.015 wt % Ti %, 0.0016 wt % Zn, 0.0003wt % Cr, 0.0019 wt % Mg, 0.0021 wt % Mn, and 0.0007 wt % Cu. The samples were polished successively with fine-grade emery papers, cleaned with acetone, washed with double-distilled water, dried, weighed, and then introduce into the test solution.

Potentiodynamic polarization measurements

The working electrode was made from Al rod that has the same composition as mentioned in the previous section. The rod was axially embedded in araldite holder to offer an active, flat, disc-shaped surface with an area of 0.785 cm^{-2}. Before each experiment, the working electrode was polished successively with fine emery paper, rinsed with acetone, washed with double-distilled water, and finally dried before it was dipped into the electrolytic cell. A platinum wire was used as a counter electrode, and a saturated calomel electrode (SCE) was used as the reference electrode to which all potentials were referred.

The electrochemical experiments are performed with a Wenking PGS95 potentiostat/galvanostat connected to a computer. The current - potential curves (I–E) were recorded with computer software (ECT). We carried out the experiments by changing the electrode potential automatically from the starting potential toward more positive values at the required scan rate until the end of the experiments.

Synthesis of MC_{10}

3-(10-Bromodecyloxy) aniline monomeric surfactant was prepared by an equimolar reaction between 3-aminophenol with 1,10-dibromodecane in the presence of sodium ethoxide. The product 3-(10-bromodecyloxy) aniline was reacted with sodium sulfite to produce MC_{10}.

Synthesis of PC_{10}

MC_{10} in a 2.0M HCl solution (25 mL) was introduced into a well-stoppered conical flask with a 250-mL capacity, followed by the addition of a required amount of potassium persulfate dissolved in a 2.0M HCl solution (25 mL) to the reaction mixture under a nitrogen atmosphere. The order of addition of substances was kept constant in all of the performed experiments. The stoppered conical flask was then placed in an automatically controlled thermostat at 25°C. The flask was shaken (50 shakings/10 s/ 15 min) for 1 h with an automatic shaker and then left for 72 h at room temperature to continue the reaction. The reaction mixture was filtered with a Buchner funnel, and the solid was washed with the distilled water and finally dried *in vacuo* at room temperature until a constant weight was reached.

Elemental and spectroscopic analyses

The elemental analysis of the prepared monomeric surfactant (MC_{10}) and its analog polymer (PC_{10}) were carried out in the microanalytical laboratory at Cairo University with oxygen flask combustions and a dosimat E415 titirator (Switzerland). The data are summarized in Table I, which shows that there was good agreement between the calculated structure and the suggested structures present in Scheme 1.

(A) Structure of monomeric surfactant (MC_{10})

(B) Structure of polymeric surfactant (PC_{10})
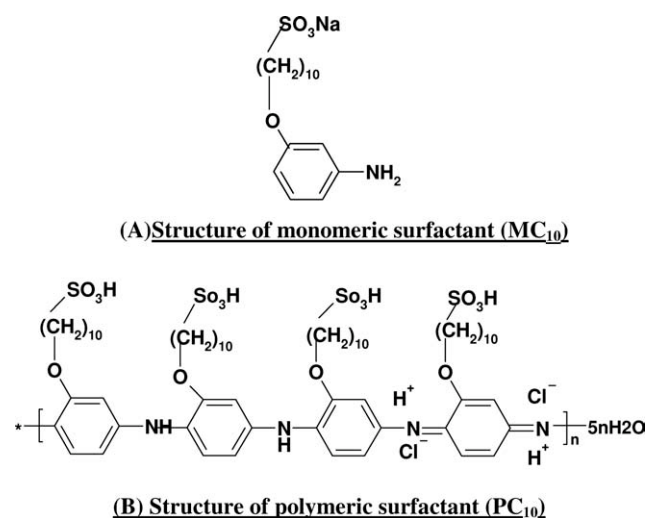
Scheme 1 Structures of (A) the monomeric surfactant and (B) the analog polymeric surfactant.

TABLE II
IR Absorption Bands and Their Assignments for MC_{10} and Its Analog PC_{10}

Wave number $(cm^{-1})^a$		Assignment[b]
MC_{10}	PC_{10}	
520^b	494^m	Bending deformation of NH in primary aromatic amines
630^{sh}	—	Out-of-plane bending deformation of CH in a 1,3-disubstituted benzene ring
751^s	755^b	In-plane rocking vibration for CH in an aliphatic chain
—	820^m	Out-of-plane bending deformation of CH in a 1,3,4-trisubstituted benzene ring
918^m	974^s	Symmetric stretching vibration for an S—O or C—N group
—	1056^w	Symmetric stretching vibration for a C—O group
1138^s	1128^w	
1204^m	—	
1326^w	1320^w	Symmetric stretching vibration for an S=O group
1437^s	1404^s	Scissoring deformation for CH in a methylene group
—	1565^m	Stretching vibration for a quinoid structure in a benzene ring
1636^b	1634^b	Stretching vibration for C=C in a benzene ring
2840^{sh}	2855^w	Symmetric stretching vibration for a CH group in an aliphatic chain
2928^m	2930^m	Asymmetric stretching vibration for a CH group in an aliphatic chain
3051^{sh}	3045^{sh}	Symmetric stretching vibration for a CH group in a benzene ring
3225^{sh}	3147^b	Stretching vibration for an OH group in an SO_3H group
3417^{sh}	—	Symmetric stretching vibration for NH in an aromatic amine
3447^b	3470^{sh}	Asymmetric stretching vibration for NH in an aromatic amine
3567^m	—	Stretching vibration for a free OH group in an SO_3H group

[a] The superscripts s, m, w, b, and sh indicate sharp, medium, weak, broad, and shoulder, respectively.
[b] These data were taken from Silverstyein et al.[27]

The infrared (IR) spectroscopy analysis of the prepared monomeric surfactant (MC_{10}) and its analog polymer (PC_{10}) was carried out in the microanalytical laboratory at Cairo University with a Jasco FTIR-430 spectrophotometer (Shimadzu) and potassium bromide disc techniques. The IR absorption bands and their assignments[27] of MC_{10} and PC_{10} are summarized in Table II. The broad absorption band appearing at 520 cm^{-1} may have been due to bending deformation of the N—H group attached to the benzene ring in the case in which the monomer appeared as a medium band at 494 cm^{-1} with slight shift in the case of the polymer. The shoulder absorption band appearing at 630 cm^{-1} was attributed to the out-of-plane deformation of CH for the 1,3-disubstituted benzene ring in the case of the monomer; it disappeared in the case of the polymer. The sharp absorption band appearing at 751 cm^{-1}, due to the rocking deformation of the methylene group in the aliphatic chain in the case of the monomer, appeared as a broad band at 755 cm^{-1}, with a slight shift in the case of the polymer. The medium absorption band at 820 cm^{-1}, which was attributed to the out-of-plane deformation of the CH group in the 1,3,4-trisubstituted benzene ring in the case of the polymer, disappeared in the case of the monomer. The medium absorption band appearing at 1565 cm^{-1} was assigned to the symmetric stretching vibration of C=C in the quinoide structure in the benzene ring and disappeared in the case of the monomer. Other absorption bands and their assignments are summarized in Table II.

Critical micelle concentrations and contact angles

The critical micelle concentrations and contact angles for the prepared monomeric surfactant (MC_{10}) and its analog polymer (PC_{10}) were measured in the hydrochloric form with different concentrations by a K100 tensiometer (KRUSS type) at 30°C.

RESULTS AND DISCUSSION

Weight loss measurements

The weight loss (mg/cm^2) of Al in a 0.5M HCl solution in the absence and presence of different concentrations of MC_{10} and its analog PC_{10} was investigated at 30°C as a function of the immersion time, and the data are graphically represented in Figure 1. The slope of the straight line relationship for each line ($mg\ cm^{-2}\ min^{-1}$) represents the corrosion rate of Al at the specified conditions. From these data, the weight loss and the corrosion rate of Al increased with the immersion time. On one hand, the dissolution of Al in the HCl solution was slow and increased with the immersion time, as indicated by the increase in weight loss with time. This may have been due to the presence of a pre-immersion hydrate Al_2O_3 film on the metal surface.[15] On the other hand, the addition of the monomeric surfactant (MC_{10}) and its analog polymer (PC_{10}) retarded the rate of dissolution and inhibited the acid corrosion of Al. The inhibition efficiency values at different inhibitor concentrations and temperatures were calculated from the following equation:
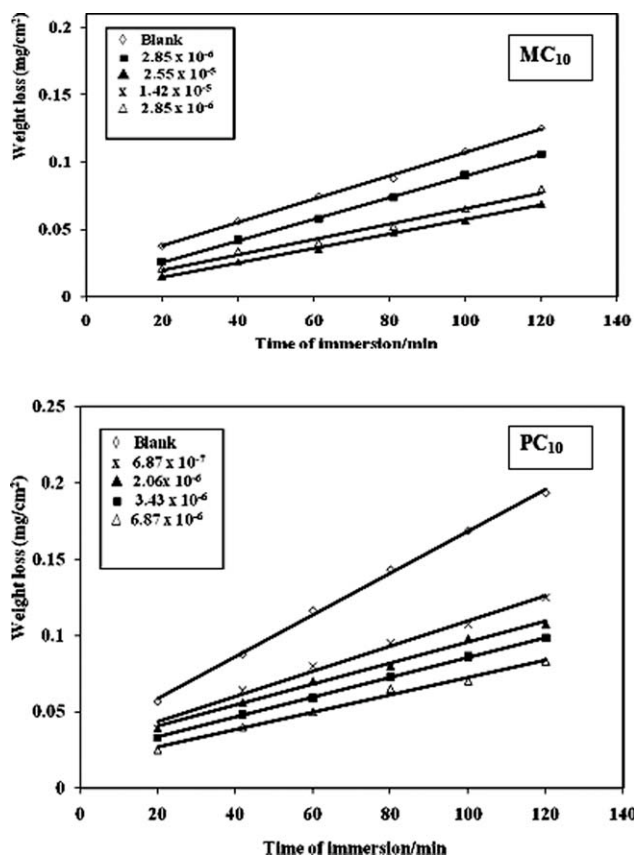
Figure 1 Weight loss versus the immersion time for Al in a 0.5M HCl solution in the absence and presence of different concentrations of MC$_{10}$ and PC$_{10}$ at 30°C.

$$\text{Inhibition efficiency } (\%) = 100 \times [1 - (W/W_0)] \quad (1)$$

where W_0 and W are the weight losses per unit of time in the absence and presence of inhibitors, respectively. The data are summarized in Table III. As shown in Table III, the inhibition efficiency of PC$_{10}$ was higher than that of MC$_{10}$. The inhibition efficiency increased with increasing concentration of two surfactants and reached a maximum value at a critical concentration (1.43 $\times$ 10^{-5} mol/L in case of MC$_{10}$ and 3.44 $\times$ 10^{-6} mol/L in case of PC$_{10}$). Beyond this critical concentration, the efficiency tended to achieve steady-state values. It was seen

that the maximum efficiency was obtained at concentrations lower than the respective critical micelle concentration (4.6 $\times$ 10^{-4} mol/L for MC$_{10}$ and 2.1 $\times$ 10^{-4} mol/L for PC$_{10}$). This means that the adsorption of these surfactants on the Al surface reached equilibrium before the formation of micelles (the aggregation of these surfactant long chains into fairly large charged units).

The *contact angle* is the angle formed when a liquid droplet is placed on the solid surface, and its values vary from 0° (perfect wetting) to 180° (complete nonwetting). The values of the contact angles for MC$_{10}$ and PC$_{10}$ at 30 °C are given in Table III. The data clearly show that the inhibition efficiency of these two inhibitors increased with the decrease in their contact angles. Moreover, it was observed that the contact angles for PC$_{10}$ were lower than these for MC$_{10}$ in all of the investigated concentrations; this confirmed that PC$_{10}$ was more effective than MC$_{10}$ in inhibiting the acid corrosion of Al.

Figure 2 shows the influence of the temperature on weight loss for Al in 0.5M HCl in the absence and presence of 10 ppm of both MC$_{10}$ and PC$_{10}$. The data show that the weight loss and the corrosion rate of the Al sample increased with increasing temperature, and the addition of both inhibitor surfactants retarded the rate of dissolution in all ranges of the investigated temperatures. This could have been due to the decrease in the strength of the adsorption process with increasing temperature; this suggested that physical adsorption may have been the type of adsorption of the inhibitor on the Al surface.

The corrosion rate (mg cm^{-2} min^{-1}) for each concentration of MC$_{10}$ and PC$_{10}$ (from 1 to 10 ppm) was calculated at different temperatures, and the logarithm of the corrosion rate was plotted against the reciprocal of the absolute temperature (1/T) for each concentration according to Arrhenius equation:[23,26]

$$\text{Logarithm of the corrosion rate} = -E_a/2.303RT + A \quad (2)$$

where E_a is the apparent effective activation energy, R is the universal gas constant, and A is the

TABLE III
Inhibition Efficiency and Contact Angle Values of Al in 0.5M HCl Solutions Containing Various Concentrations of MC$_{10}$ and Its Analog PC$_{10}$ at 30°C

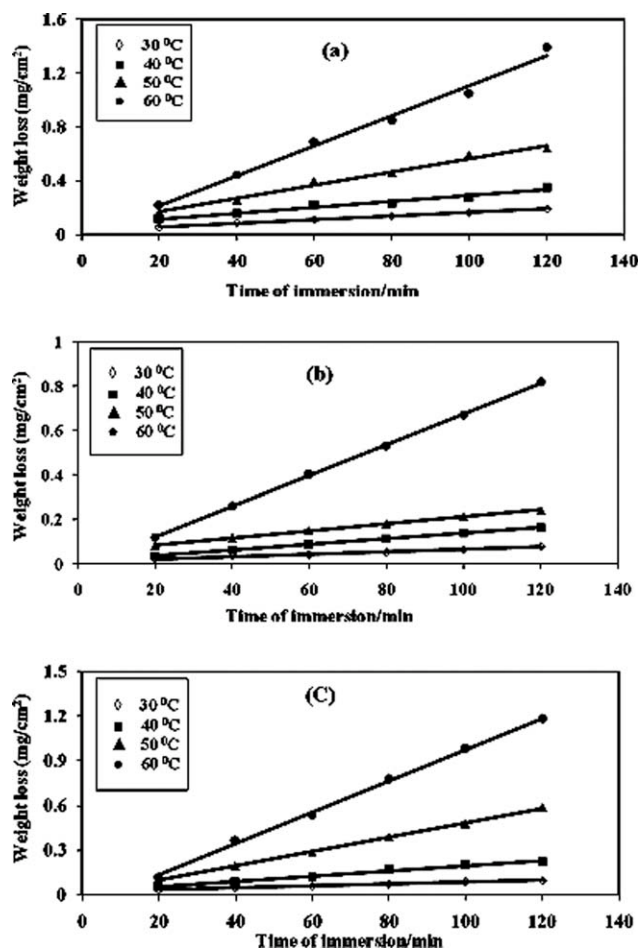| | Inhibition efficiency (%) | | | | Contact angle (°) | |
| | Weight loss | | Polarization | | | |
Concentration (ppm)	MC$_{10}$	PC$_{10}$	MC$_{10}$	PC$_{10}$	MC$_{10}$	PC$_{10}$
1	26.2	32.7	26.6	34.9	62.20	29.07
3	42.2	46.7	44.0	50.8	49.01	25.97
5	48.1	59.3	49.9	58.3	00.00	8.52
10	47.0	53.0	46.4	54.0	22.90	10.33

Figure 2 Weight loss versus the immersion time for Al in a 0.5M HCl solution (a) in the absence of MC_{10}, (b) in the presence of 10 ppm MC_{10}, and (c) in the presence of 10 ppm PC_{10} at different temperatures.

Arrhenius pre-exponential factor. The values of E_a in the absence and presence of each concentration of both surfactants were calculated and are tabulated in Table IV.

An alternative formula of the Arrhenius equation is the transition state equation:[23,26]

$$\text{Rate} = RT/Nh \, \exp(\Delta S^0/R) \, \exp(-\Delta H^0/RT) \quad (3)$$

where h is Planck's constant, N is Avogadro's number, ΔS^0 is the entropy of the activation, and ΔH^0 is the enthalpy of activation. The plot of the log(corrosion rate/T) versus $1/T$ gives a straight line with a slope of $(-\Delta H^0/2.303R)$, from which the values of ΔH^0 were calculated; they are listed in Table IV.

The data in Table IV reveal that the addition of both surfactant inhibitors enhanced the values of both E_a and ΔH^0. This enhancement may have been due to the adsorption of surfactant inhibitors on the Al surface and increased the energy barrier of the corrosion reaction as the concentrations of the inhibitors increased. This suggests that the process was activation-controlled. The activation energy value of 79.4 kJ/mol for the HCl inhibitor systems suggested the fact that the inhibitors were physically adsorbed on the Al surface, which was in agreement with some earlier reports.[28–31]

Potentiodynamic polarization measurements

Figure 3 shows the effect of different concentrations of MC_{10} and PC_{10} on the potentiodynamic cathodic and anodic polarization curves for Al in a 0.5M HCl solution with a scan rate of 25 mV/s at 30°C, whereas Figure (4) illustrates the influence of temperature on the potentiodynamic cathodic and anodic polarization curves of Al in a 0.5M HCl containing 10 ppm of both MC_{10} and PC_{10}. The data clearly show that the addition of MC_{10} and PC_{10} enhanced both the anodic and cathodic overpotential and decreased the corresponding partial anodic (dissolution of the metal) and partial cathodic (evolution of hydrogen) current densities. The addition of each inhibitor decreased the values of I_{corr} is corrosion current; this confirmed the inhibition of the corrosion process. Moreover, the corrosion potentials were displayed to more positive values in the presence of the inhibitors; this revealed that these surfactants predominately acted as anodic inhibitors.

The electrochemical parameters (I_{corr}, E_{corr}, corrosion potential, β_c, and β_a are cathodic and anodic Tafel slope respectively) and the corrosion rate associated with the corrosion of Al in the absence and presence of different concentrations of MC_{10} and PC_{10} at different temperatures are listed in Tables III, V, and VI, respectively.

TABLE IV
Effects of the Concentrations of MC_{10} and Its Analog PC_{10} on the Thermodynamics of the Dissolution Process of Al in a 0.5M HCl Solution

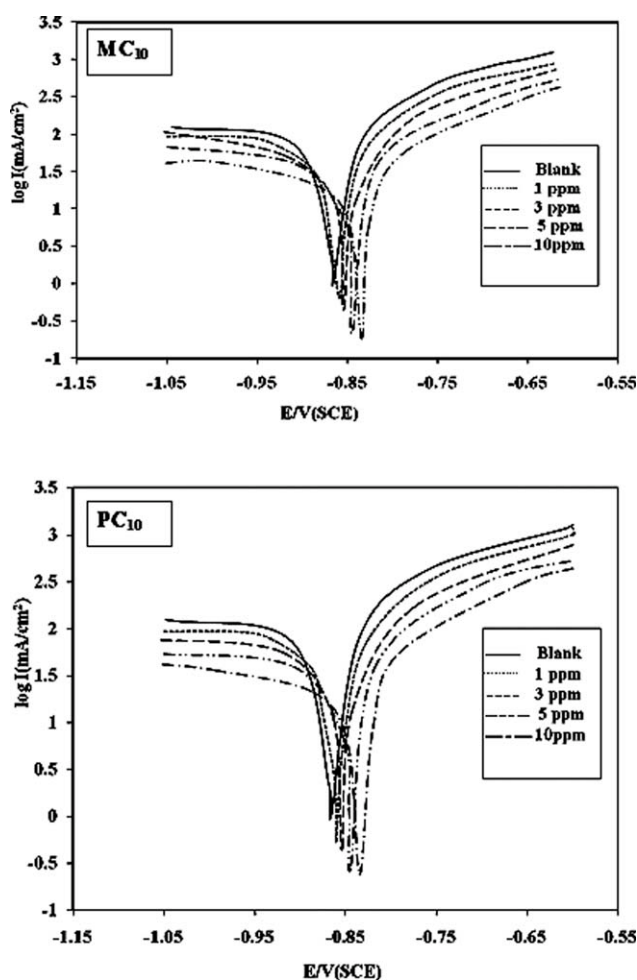| Concentration (ppm) | E_a (kJ/mol) | | | | ΔH^0 (kJ/mol) | | | |
| | Weight loss | | Polarization | | Weight loss | | Polarization | |
	MC_{10}	PC_{10}	MC_{10}	PC_{10}	MC_{10}	PC_{10}	MC_{10}	PC_{10}
Blank	57.4	57.4	57.3	57.3	55.5	55.5	54.7	54.7
1	62.33	66.7	61.7	65.1	59.61	63.51	59.2	62.2
3	67.89	70.9	68.7	71.3	64.63	68.95	66.1	68.7
5	70.22	79.1	70.1	79.4	68.82	78.90	65.4	75.8
10	69.31	78.6	68.9	74.8	66.95	77.00	67.4	71.4

Figure 3 Effects of the MC$_{10}$ and PC$_{10}$ concentrations on the cathodic and anodic polarization of Al in a 0.5M HCl solution at a scan rate of 25 mV/s at 30°C.

It was seen that the inhibition efficiency increased with increasing surfactant concentration up to critical concentrations but decreased with increasing temperature. The presence of these inhibitors did not significantly change the values of cathodic and anodic Tafel lines slopes. These results indicate that these inhibitors acted by simply blocking the available surface area for the corrosion process. In other words, each inhibitor decreased the surface area for corrosion without affecting the mechanism of the corrosion
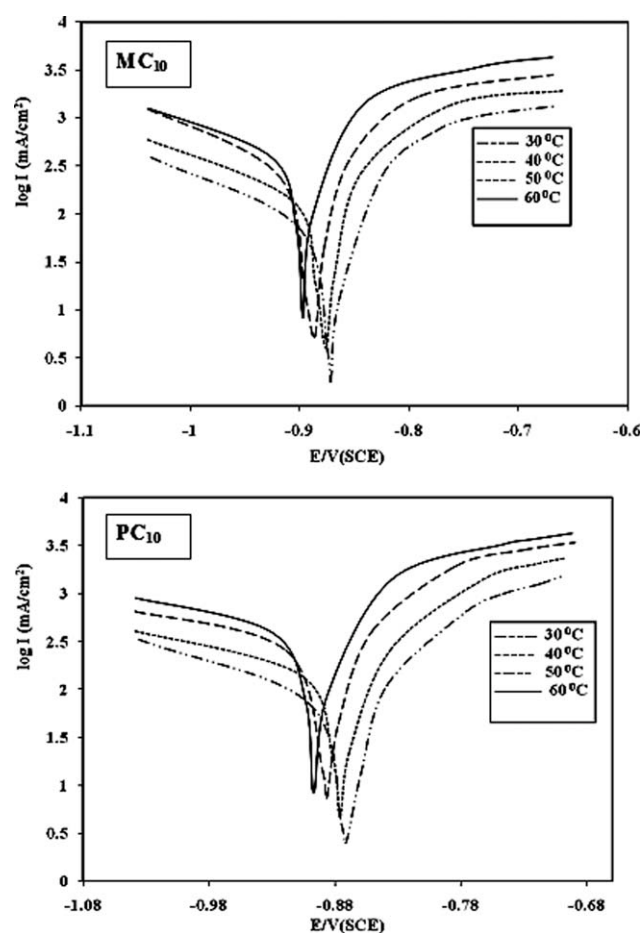

Figure 4 Effects of the temperature on the cathodic and anodic polarization of Al in a 0.5M HCl solution in the presence of 10 ppm MC$_{10}$ and PC$_{10}$ at a scan rate of 25 mV/s.

process and only caused inactivation of a part of the Al surface with respect to the corrosive medium.

Adsorption isotherm

To get more information about the mode of adsorption of these inhibitors on the Al surface at different temperatures, the obtained data from the two different techniques were tested with several adsorption isotherms, and it was found that the experimental data fit the Langmuir adsorption isotherm, which is given by the following equation:[32]

TABLE V
Electrochemical Parameters Associated with Polarization Measurements for Al in a 0.5M HCl Solution in the Absence and Presence of Different Concentrations of MC$_{10}$ and Its Analog PC$_{10}$ at 30°C

Concentration (ppm)	MC$_{10}$				PC$_{10}$			
	E_{corr} versus SCE (mV)	I_{corr} (μA/cm^2)	β_a (mV/dec)	$-\beta_c$ (mV/dec)	E_{corr} versus SCE (mV)	I_{corr} (μA/cm^2)	β_a (mV/dec)	$-\beta_c$ (mV/dec)
Blank	−0.82	95.22	−0.349	0.044	−0.82	95.22	−0.349	0.044
1	−0.721	69.82	−0.34	0.109	−0.77	62.00	−0.307	0.047
3	−0.71	52.84	−0.347	0.121	−0.79	46.83	−0.37	0.075
5	−0.82	47.7	−0.268	0.103	−0.788	39.83	−0.34	0.066
10	−0.75	50.98	−0.319	0.084	−0.56	43.82	−0.614	0.81

Electrochemical Parameters Associated with Polarization Measurements for Al in a 0.5M HCl Solution in the Presence of 10 ppm MC$_{10}$ and Its Analog PC$_{10}$ at Different Temperatures

	MC$_{10}$				PC$_{10}$			
T (K)	E_{corr} versus SCE (mV)	I_{corr} ($\mu A/cm^2$)	β_a (mV/dec)	$-\beta_c$ (mV/dec)	E_{corr} versus SCE (mV)	I_{corr} ($\mu A/cm^2$)	β_a (mV/dec)	$-\beta_c$ (mV/dec)
303	−0.75	50.98	−0.319	0.084	−0.56	43.82	−0.614	0.81
313	−0.76	216.6	0.168	1.04	−0.97	198.6	−0.55	0.8
323	−0.77	383.1	−0.77	−0.163	−0.98	374.6	−0.43	0.11
333	−1.07	558.6	−0.39	0.164	−1.01	541.1	−0.54	0.16

$$C_i/\theta = 1/K_{ads} + C_i \quad (4)$$

where C_i is the concentration of the inhibitor in a bulk solution, θ is the surface coverage (θ = Inhibition efficiency/100), and K_{ads} is the adsorption equilibrium constant.

Figure 5 represents curves fitting of MC$_{10}$ and PC$_{10}$ with data obtained from the potentiodynamic polarization measurements. Similar results were obtained from the weight loss technique.

The Frumkin adsorption isotherm was also found to fit well with the experimental data obtained from the weight loss technique for both MC$_{10}$ and PC$_{10}$.

The adsorption isotherm relationship of Frumkin is represented by the following equation:[33]

$$\ln \theta/C_i(1 - \theta) = \ln K_{ads} + 2a\theta \quad (5)$$

where a is the lateral interaction term describing the molecular interactions in the adsorption layer and the heterogeneity of the surface and measure for the steepness of the adsorption isotherm. The more positive the value of a is, the steeper the adsorption isotherm is. Curve-fitting of the weight loss data for MC$_{10}$ and PC$_{10}$ are graphically represented in Figure 6. Similar results were obtained from the data of the potentiodynamic technique.
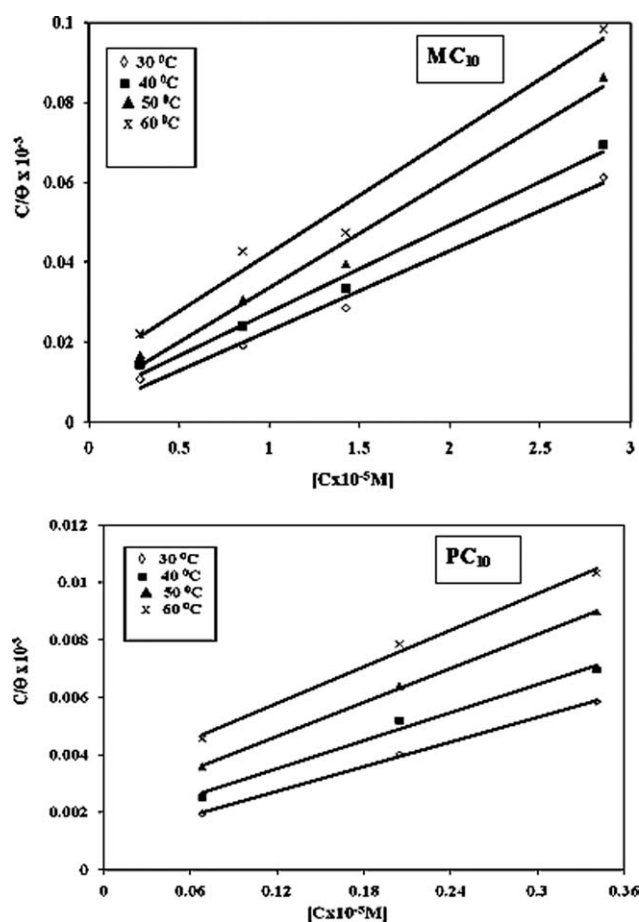

Figure 5 Langmuir adsorption isotherms of MC$_{10}$ and PC$_{10}$ based on polarization data at different temperatures.
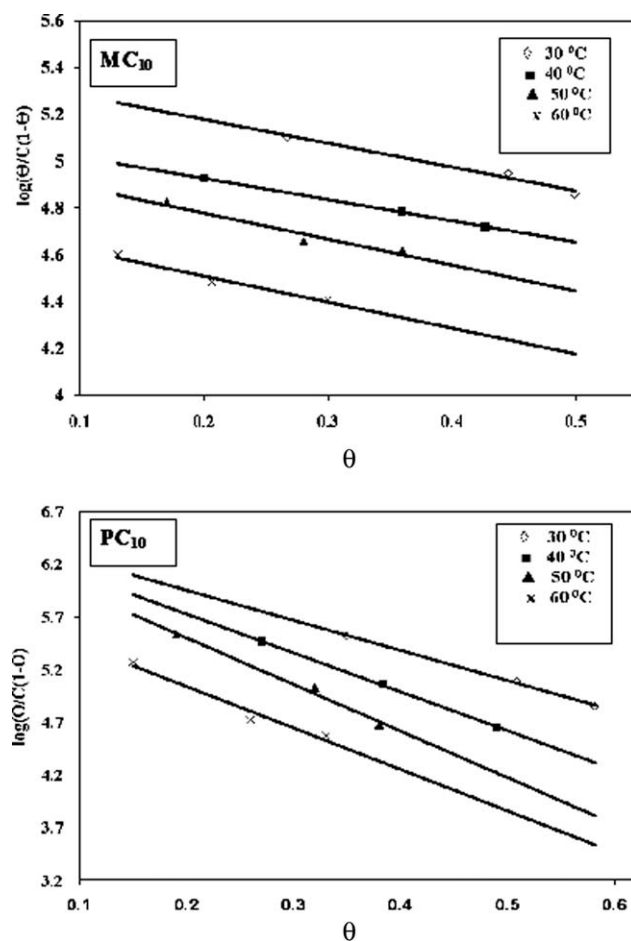

Figure 6 Frumkin adsorption isotherms of MC$_{10}$ and PC$_{10}$ based on weight-loss data at different temperatures.

TABLE VII
Thermodynamic Parameters of the Adsorption Process Based on Frumkin Isotherm

Technique	MC$_{10}$			PC$_{10}$		
	ΔH_{ads} (kJ/mol)	ΔS_{ads} (kJ mol^{-1} K^{-1})	$-\Delta G_{ads}$ (kJ/mol)	ΔH_{ads} (kJ/mol)	ΔS_{ads} (kJ mol^{-1} K^{-1})	$-\Delta G_{ads}$ (kJ/mol)
Weight loss	−48.63	−0.052	32.87	−51.95	−0.0491	37.08
Polarization	−45.76	−0.048	31.258	−52.85	−0.0504	37.59

The parameters were obtained with Frumkin isotherms based on weight-loss and polarization data for Al in a 0.5M HCl solution.

G_{ads}, Free Energy of the adsorption process.

The adsorption thermodynamic parameters [the enthalpy of the adsorption process (ΔH_{ads}) and the entropy of the adsorption process (ΔS_{ads})] for the surfactant adsorption on the Al surface in 0.5M HCl at different temperatures were determined from the slopes and intercepts of the lines of adsorption equilibrium constant (log K_{ads}) versus $1/T$ plots with the following equation:

$$\text{Log } K_{ads} = -\Delta H_{ads}/2.303RT + \Delta S_{ads}/2.303R \quad (6)$$

The calculated values for ΔH_{ads} and ΔS_{ads} are listed in Table VII. The calculated values of ΔG_{ads} were low; this suggested that the nature of the inhibitor adsorption was mainly physical adsorption, and their negative sign indicated spontaneous interaction of the inhibitor with the Al surface.[34] The negative value of ΔH_{ads} indicated that the adsorption of the inhibitors on Al surface was an exothermic process. The values of ΔH_{ads} and ΔS_{ads} were characteristic of the occurrence of a replacement process between the inhibitor species and adsorbed water molecules from the surface of the metal during the adsorption of the inhibitor compound on the metal surface.[35]

CONCLUSIONS

The addition of MC$_{10}$ and its analog PC$_{10}$ inhibited the corrosion of Al in a 0.5M HCl solution.

The inhibition efficiency of the polymeric surfactant was higher than that of the monomeric surfactant, and the inhibition efficiency increased with increasing inhibitor concentration but decreased with increasing temperature.

The data obtained from the weight loss and potentiodynamic polarization techniques were in good agreement with each other and fit well with the Langmuir and Frumkin isotherms.

References

1. Ovari, F.; Tomcsanyi, L.; Turmezey, T. Electrochim Acta 1988, 33, 323.
2. Tomcsanyi, L.; Varga, K.; Bartik, I.; Horanyi, G.; Maleczki, E. Electrochim Acta 1989, 34, 855.
3. Stevanovic, R. M.; Despic, A. R.; Drazic, D. M. Electrochim Acta 1988, 33, 397.
4. Frers, S. E.; Stefenel, M. M.; Mayer, C.; Chierchie, T. J Appl Electrochem 1990, 20, 996.
5. Rozenfeld, I. L. Corrosion Inhibitors; McGraw-Hill: New York, 1981; p 182.
6. Desai, M. N.; Thakar, B. C.; Chiaya, P. M.; Gandi, M. H. Corros Sci 1976, 16, 9.
7. Hackerman, N.; Makrides, A. C. Ind Eng Chem 1954, 46, 523.
8. Granese, S. L.; Rosales, B. M. Proc Eur Symp Corros Inhibitors 1990, 9, 73.
9. Khaled, K. F.; Al-Qahtani, M. M. J Mater Chem Phys 2009, 113, 150.
10. El-Awady, Y. A.; Ahmed, A. I. J Ind Chem 1985, 24A, 601.
11. Moussa, M. N. H.; Taha, F. I. M.; Gouda, M. M.; Singab, G. M. Corros Sci 1976, 16, 379.
12. Issaa, I. M.; Moussa, M. N. H.; Ghondoura, M. A. A. Corros Sci 1973, 13, 79.
13. Bracher, D.; Mercer, A. D. Br Corros J 1968, 3, 120.
14. Maitra, A.; Barua, S. Corros Sci 1974, 14, 587.
15. Osman, M. M.; Abdel Rehim, S. S. J Mater Chem Phys 1998, 53, 34.
16. Gomma, G. K.; Wahdan, M. H. J Mater Chem Phys 1995, 39, 209.
17. Hackerman, N.; Sudbury, J. D. J Electrochem Soc 1950, 94, 4.
18. Hackerman, N. Corrosion 1962, 18, 332t.
19. Zhao, T.; Mu, G. Corros Sci 1999, 41, 1937.
20. Karlsson, P. M.; Baeza, A.; Palmqvist, A. E.; Holmberg, K. Corros Sci 2008, 50, 2282.
21. Abd El Rehim, S. S.; Hassan, H. H.; Amin, M. A. Corros Sci 2004, 46, 5.
22. Abd El Rehim, S. S.; Hassan, H. H.; Amin, M. A. J Mater Chem Phys 2001, 70, 64.
23. Sayyah, S. M.; Abd El-Rehim, S. S.; El-Deeb, M. M. Int J Polym Mater 2001, 49, 59.
24. Jianguo, Y.; Lin, W.; Otieno-Alego, V.; Schweinsberg, D. Corros Sci 1995, 37, 37.
25. Abo El-Khair, B. M. Corros Prev Control 1983, 30, 15.
26. Abd El Rehim, S. S.; Sayyah, S. M.; El-Deeb, M. M.; Kamal, S. M.; Azooz, R. E. J Mater Chem Phys 2010, 123, 20.
27. Silverstyein, R. M.; Bassler, C. G.; Morill, T. C. Spectroscopic Identification of Organic Compounds; Wiley: New York, 1974.
28. Elewady, G. Y.; El-Said, I. A.; Fouda, A. S. Int J Electrochem Sci 2008, 3, 177.
29. Abiiola, O. K.; Oforka, N. C. Corros Sci Eng 2002, 3, 21.
30. Damaskin, B. B. Adsorption of Organic Compounds on Electrodes; Plenum: New York, 1971; p 221.
31. Ebenso, E. E. J Mater Chem Phys 2003, 79, 58.
32. Migahed, M. A.; Azzam, E. M.; Al-Sabagh, A. M. Mater Chem Phys 2004, 85, 273.
33. Frumkin, A. N. Z Phys Chem 1915, 116, 166.
34. Ateya, B.; El-Anadouli, B.; El-Nizamy, F. Corros Sci 1984, 24, 509.
35. Iampinen, M. J.; Fomino, M. J Electrochem Soc 1993, 140, 3537.